

Valorization of Microcrystalline Cellulose using Heterogeneous Protonated Zeolite Catalyst: An experimental and kinetics approach

Samuel Kassaye

Kansas State University

Dinesh Gupta

Indian Institute of Technology

Kamal. K. Pant

Indian Institute of Technology Delhi

Sapna Jain (✉ sjain@alasu.edu)

Alabama State University <https://orcid.org/0000-0002-0164-1446>

Research Article

Keywords: Microcrystalline cellulose, Ionic liquid, Hydrolysis, Kinetic modelling

Posted Date: April 14th, 2021

DOI: <https://doi.org/10.21203/rs.3.rs-381188/v1>

License:  This work is licensed under a Creative Commons Attribution 4.0 International License.

[Read Full License](#)

1 Valorization of Microcrystalline Cellulose using Heterogeneous Protonated 2 Zeolite Catalyst: An experimental and kinetics approach

3
4 Samuel Kassaye¹, Dinesh Gupta¹, Kamal. K. Pant¹, Sapna Jain*²

5
6 ¹Department of Chemical Engineering, Indian Institute of Technology Delhi, Hauz Khas, New Delhi
7 110016, India

8 ²Department of Physical Science, Alabama State University, Montgomery Al 36104, USA

9 *Author for correspondence: Tel.: 334-467-7083

10 *E-mail address: sjain@alasu.edu (Sapna Jain)

11 12 **Abstract**

13 This study aims to valorize microcrystalline cellulose (MCC) using protonated zeolite catalysts
14 such as (H-ZSM-5) and Cr/H-ZSM-5 (5 %) in ionic liquid. The catalytic effect in synergy with 1-
15 butyl-3-methylimidazolium Chloride ([BMIM] Cl) ionic liquid was studied in detail. The total
16 reducing sugar (TRS) was determined using 3, 5-dinitrosalicylic acid (DNS) array method. The
17 catalysts were characterized using techniques such as Fourier transform infrared (FT-IR), X-ray
18 diffraction analysis (XRD), temperature-programmed desorption of ammonia (NH₃-TPD), and
19 BET-surface area analyzer. H-ZSM-5 effectively depolymerized cellulose with a maximum yield
20 of 70% total reducing sugar (34% glucose, 8% fructose, and 4.5% 5-HMF) Cr/H-ZSM-5 catalyst
21 dehydrates fructose to 5-HMF with a yield of 53%. The use of ionic liquid significantly reduced
22 the activation energy of formation and decomposition. The activation energy determined in
23 cellulose hydrolysis was 85.83 KJ mol⁻¹ for a reaction time of 180 min while the decomposition
24 energy was found to be 42.5 kJ mol⁻¹.

25
26 **Keywords:** Microcrystalline cellulose, Ionic liquid, Hydrolysis, Kinetic modelling

27 **1. Introduction**

28 Efficient and Economic conversion of lignocellulosic biomass (LCB) to value-added chemicals in
29 integrated biorefinery is believed to reduce the dependency on a nonrenewable resource such as
30 fossil fuel. LCB is a promising feedstock for the biorefinery industry to produce biofuel and
31 valuable chemicals from renewable sources [1]. Successful utilization of biomass demands the
32 effective conversion of the cellulosic portion of LCB to develop integrated biorefinery to produce
33 biofuel and chemicals economically. The hydrolysis of cellulose strongly depends on its properties
34 such as degree of polymerization and crystallinity. The utilization of lignocellulosic biomass
35 depends on the level of success achieved on hydrolysis of the cellulose into its monomeric form,
36 glucose [2]. However, cellulose is the most recalcitrant and well-known crystalline biopolymer
37 due to its extensive intra and inter-hydrogen bonding network. Cellulose is a structurally linear
38 polymer composed of glucose monomers joined together by β -1, 4-glycosidic linkage [3].
39 Therefore, it is difficult to dissolve and subsequently hydrolyze cellulose using conventional
40 organic solvents including water and ethanol [4] [5].

41 The hydrolysis of cellulosic biomass is carried out using an enzymatic approach accompanied by
42 a high glucose yield at moderate reaction conditions. Enzymatic hydrolysis has several
43 disadvantages related to the high cost of enzymes, limited cellulose conversion, and scalability
44 challenges [3]. Hydrolysis of cellulose using acidic catalysts such as liquid acids including mineral
45 and organic acids is another alternative option [6]. Mineral acids are highly efficient in breaking
46 β -1,4-glucosidic linkage [7] [8]. However, this method has several drawbacks: reaction product
47 decomposition, difficulty in the product, and catalyst separation. Mineral acid catalysts are also
48 known to cause reactor corrosion, costly post- treatment, challenges in recycling catalysts and
49 consumption of a large amount of neutralizing agents [9] [10]. As a result, attempts are underway

50 to apply solid acid catalysts to convert lignocellulosic biomass to bio-chemicals. The application
51 of ionic liquids further improves this approach. Some selected ionic liquids have inherent
52 characteristics to dissolve cellulose and disrupt the hydrogen bonding network effectively.

53 Ionic liquids (ILs) are low melting point organic salts that can be utilized both as solvents and
54 catalysts to convert lignocellulosic biomass [11]. The suitability of ILs for biomass utilization is
55 attributed mainly to their tunable Physico-chemical properties such as viscosity, polarity, and thermal
56 stability. ILs act as non-volatile polar solvents and it can dissolve the complex cellulosic materials. The
57 use of ILs allows production flexibility with high efficiency while eliminating the use of undesirable
58 volatile solvents. In this regard, solid acid catalysts such as zeolites, ion exchange resins, and zirconia
59 are considered an alternative chemo-catalytic approach for cellulose depolymerization. The use of
60 zeolite based solid acid catalysts have tremendous advantages compared to homogeneous catalysts
61 such as easy separation, recyclability, and adjustable surface acidity [12].

62 Zeolite catalysts have been modified and used in industrial processes as milestones in history and
63 have brought profound changes in the petrochemicals industry. For example, Zeolite Y's use in the
64 Fluid Catalytic Cracking (FCC) process significantly increased fuel production efficiency. HZSM-
65 5, which has 8 to 10-member ring with pore-size between 0.5 and 56 nm, is well suited for bio-
66 refinery. However, cellulose insolubility in aqueous media has been the foremost hurdle to apply
67 zeolites as solid acid catalysts due to solid-solid formation which limits mass transfer and
68 reactivity. However, ionic liquids with unique properties to dissolve cellulose and reduce its
69 crystallinity have been a choice to convert cellulose to value-added chemicals [13] [14].

70 Zeolites inherently possess both Bronsted and Lowry as well as Lewis acid sites. These acidic sites
71 help catalyze and promote hydrolysis of cellulose, isomerization of glucose, and fructose
72 dehydration [15]. H-ZSM-5 catalyst has been the choice of this study due to its inherent properties,

73 such as strong and active acid sites suitable for a catalyst with a porous structure and larger surface
74 area. These properties enhance and facilitates the depolymerization of cellulose to produce bio-
75 chemicals. In this research work, the catalytic effects of H-ZSM-5 and Cr/H-ZSM-5 (5 %) were
76 studied to depolymerize MCC. The experimental results showed that the synergy between ionic
77 liquid and H-ZSM-5 improved cellulose conversion and the yield of the desired bio-chemicals.
78 Results showed that this approach generated a 70% yield of total reducing sugar (34% glucose,
79 8% fructose and 4.5% 5-HMF) at moderate temperature and atmospheric pressure. Besides, ionic
80 liquid presence significantly reduced the activation energy of the formation and decomposition of
81 sugar.

82 **2. Materials and Methods**

83 **2.1 Materials**

84 All the chemicals used were of analytical grade (purity 99.9%). Microcrystalline cellulose extra
85 pure, the average particle size of 90 μ m is purchased from Alfa Aesar (A Johnson Matthey
86 Company, Heysham, Lancashire, United Kingdom). As reported in our previous research work
87 [16], the original MCC's initial crystallinity index was found to be 76%, which reduced to 42%
88 due to the influence of the ionic liquid. 1-Chlorobutane, N-methyl imidazole, toluene, acetone
89 acetonitrile, ethyl acetate, 3,5-dinitrisalicylic acid, sodium hydroxide, sodium potassium tartrate
90 phenol, acetonitrile, cellulose and isopropanol were purchased from Fisher Scientific (Anand
91 Bhuvan, Princess Street Mumbai, India), H-ZSM-5 with Si/Al ratio of 30 was obtained from Sud-
92 chemie India. [BMIM] Cl ionic liquid was prepared and characterized as reported in our previous
93 work [16].

94 **2.2 Methods**

95 **2.2.1 Catalysts Synthesis and Characterization**

96 Chromium-impregnated H-ZSM-5 (Cr/H-ZSM-5) catalyst was prepared using wet impregnation
97 method in which H-ZSM-5 was mixed with chromium precursor ($\text{CrCl}_3 \cdot 6\text{H}_2\text{O}$) in 50 ml distilled
98 water [17]. The mixture was stirred vigorously for 3 h at 80 °C and then, the excess solvent was
99 removed by rotary evaporator at reduced pressure. Subsequently, the sample was dried overnight
100 at 120 °C and calcined at 500 °C for 5 h. The catalysts were characterized using FTIR, XRD, BET
101 surface area, ammonia TPD and TGA. The thermal properties of both catalysts were studied using
102 thermo-gravimetric analysis (TGA). The analysis was performed using nitrogen gas as a purge gas
103 at a flow rate of 30 ml per min with a heating rate of 20 °C per min from 30 to 1,000 °C.

104 Temperature programmed desorption of ammonia (NH_3 -TPD) was performed to determine the
105 total acid strength and acid site distribution on the surface of both catalysts using the Micromeritics
106 Pulse Chemisorb 2720 instrument. The chemisorb instrument is equipped with a quartz reactor
107 and a thermal conductivity detector (T.C.D). The sample catalyst (0.2 g) was pre-treated at 250 °C
108 for 2h with a continuous flow of pure helium gas to remove the moisture content at room
109 temperature. The sample was then saturated with 10% ammonia gas for adsorption for 1h. After
110 complete saturation, physisorbed ammonia was removed by flowing helium for 30min. The TPD
111 was carried out in a stream of helium gas, raising the temperature from 50° C to 980 °C at the rate
112 of 10 °C per min. The desorption process of ammonia was monitored using a T.C.D detector and
113 the amount of total desorbed ammonia was obtained from the integrated peak area of the TPD
114 profiles relative to the calibration curve.

115 **2.2.2 Catalytic Hydrolysis**

116 The hydrolysis of MCC was performed using a batch reactor of 250ml size where the dissolution
117 of MCC was performed in [BMIM] Cl ionic liquid with 1:20 w/w proportion. The stirring was

118 carried out continuously for 30 min until the mixture turns homogeneous. Then, 5 mL of distilled
119 water and H-ZSM-5 (1:2 w/w ratio of MCC to H-ZSM-5) was added and the solvent was refluxed
120 back to the reactor using a condenser. On the completion of the reaction time, the reaction mixture
121 was quenched using an ice bath. Then, the catalyst and the hydrolysate were separated using
122 vacuum filtration process. The hydrolysate was centrifuged at 10,000 rpm for 10min and then
123 stored in a refrigerator for further analysis.

124 **2.2.3 Hydrolysis Product Analysis**

125 The samples were analyzed using dinitrosalicylic acid (DNS) reagent in UV-Vis Spectroscopy
126 for TRS yield while HPLC was used to determine the yield of sugars and dehydration products.
127 DNS analysis hydrolysate was mixed with DNS reagent in 1:2 v/v ratio and boiled for 10 minutes
128 in a water bath. The resulting solution was cooled using an ice bath and the analysis was carried
129 out by measuring the absorbance of the sample using UV-Vis spectroscopy (CARY 100Conc) at
130 540 nm wavelength. The total reducing sugar yield was determined from the calibration curve
131 formed using four-point concentration of standard glucose solutions. The yield of TRS was
132 calculated using Equation 1.

$$133 \quad \text{TRS Yield (\%)} = \frac{\text{Mass of reducing sugar} \times \frac{162}{180} \times 100}{\text{Mass of dry cellulose}} \quad (1)$$

134 Fructose, glucose, and 5-HMF were analyzed using high-performance liquid chromatography
135 (HPLC). The HPLC analysis was performed using Agilent technology 1200 infinity equipped with
136 Bio-Rad Aminex HPx-87H 300 x 7.8 mm columns, UV-detector for sugar dehydration product
137 and RI detector for sugar products. The eluent was 5mM sulphuric acid with a flow rate of 0.6 ml
138 per minute and the injection volume was 20 μ l. The identification of products in the sample was

139 performed using a pure form of the products to determine retention time and calibration curve
140 formation. The 5-HMF was calculated as given below in Equation 2.

$$141 \quad 5\text{-HMF Yield (\%)} = \frac{\text{moles of 5-HMF produced} \times 100}{\text{moles of cellulose feed}} \quad (2)$$

142 **3. Result and Discussion**

143 **3.1 Catalysts Characterization**

144 The catalyst was characterized using FTIR, XRD, BET surface area, ammonia TPD and TGA
145 analysis as discussed below.

146 **3.1.1 FT-IR Analysis**

147 H-ZSM-5 and Cr/H-ZSM-5 catalysts were characterized by FT-IR method to study the effect of
148 chromium metal incorporation into the framework structure of the H-ZSM-5 catalyst. The FTIR
149 spectra of H-ZSM-5 and Cr / H-ZSM-5 catalysts range between 500 and 2000 cm^{-1} shown in Figure
150 1. The result shows that the position of sensitive structural bands of H-ZSM-5 and Cr/H-ZSM-5
151 catalysts have similar positions. This implies that chromium metal incorporation into the zeolite
152 structure was insignificant to alter the basic zeolite structure and functional groups. The internal
153 vibrations of SiO_4 and AlO_4 are represented by the absorption bands at 1,088 and 810 cm^{-1} ,
154 respectively [18]. Similarly, the bands near 540 and 1225 cm^{-1} are assigned to the double ring
155 vibration and asymmetric stretching.

156

157 **3.1.2 XRD Analysis**

158 Figure 2 shows the XRD-spectra pattern of H-ZSM-5 and Cr/H-ZSM-5. The XRD data analysis
159 was used to study the effect of chromium metal incorporation on the framework structure of the
160 H-ZSM-5 catalyst. The intensity and the number of diffraction peaks of both catalysts were similar
161 and there is no indication of significant change in the XRD pattern. However, the peak of the Cr/H-
162 ZSM-5 catalyst has shown a slight shift to the left. According to the Bragg equation, this shift in
163 the peak of Cr/H-ZSM-5 catalyst is attributed to the increase in interplanar d-spacing due to
164 chromium metal presence in the framework [19]. This indicates that the bigger lattice parameters
165 representing the inclusion of atoms of different diameters. However, extra diffraction peaks were
166 not observed representing uniform dispersion of chromium throughout the zeolite framework
167 structure [20].

168 **3.1.3 BET Analysis**

169 The BET surface area analysis for H-ZSM-5 and Cr/H-ZSM-5 is given in Table 1. According to
170 the results, the surface area of H-ZSM-5 decreased after the impregnation of chromium metal.
171 Impregnation of chromium metal to H-ZSM-5 led to a decrease in surface area from 270 to 248
172 m^2g^{-1} due to the partial pores blocking H-ZSM-5 structural support by chromium metal [21].

173 **3.1.4 Ammonia –TPD Analysis**

174 The acid site property of the catalysts was studied using temperature-programmed desorption of
175 ammonia (Ammonia-TPD). As presented in Figure 3, the catalysts' acid site distribution was
176 determined using the desorption peaks. The result showed the effect of chromium metal
177 impregnation into the framework structure on the acidity of H-ZSM-5. The entire surface acid sites
178 of Cr/H-ZSM-5 qualitatively increased compared to H-ZSM-5 implying the presence of additional
179 acid sites due to the inclusion of chromium into the H-ZSM-5 structure [22]. For H-ZSM-5, the

180 low-temperature peak was observed at a temperature between 150 - 300 °C while the high-
181 temperature peak was observed in between 300 - 500 °C representing the low and high desorption
182 peaks, respectively.

183 Similarly, Cr/H-ZSM-5 catalyst showed the acid sites distribution at a low temperature of 200 -
184 300 °C while the high-temperature peak at 350 - 650 °C. The peak at low and high temperature
185 indicates the presence of weak and strong acid sites, respectively. In general, the incorporation of
186 chromium metal into the frameworks of H-ZSM-5 increased both the strong and the weak acid
187 sites. However, the effect on strong acid sites is more significant than the weak acid sites which
188 are consistent with the literature [21].

189 **3.2 Hydrolysis of MCC**

190 In a preliminary study, hydrolysis of MCC was performed in the absence of H-ZSM-5 catalyst,
191 [BMIM] Cl and prior dissolution for a reference purpose. Compared with the reference, the
192 hydrolysis reaction was significantly influenced by the prior dissolution in ionic liquid and the
193 catalytic amount of H-ZSM-5. In this condition, 70% maximum yield of TRS was achieved at a
194 temperature of 180 oC, reaction time of 180 min, and catalyst to substrate loading ratio of 2:1
195 (w/w). The high sugar yield from the prior dissolution process is attributed to the structural change
196 from microcrystalline to amorphous cellulose due to the ionic liquid effect [5]. The ionic liquid
197 used was potent enough to break the hydrogen bonding networks which hold the cellulose strand
198 together. As a result, cellulose's crystallinity reduced significantly, facilitating the accessibility of
199 cellulose to the acid sites of the H-ZSM-5 catalyst. The exposure of the acid sites breaks the
200 glycosidic bonds of the glucose monomers. In similar experimental work under identical
201 conditions except for the absence of catalyst, hydrolysis reaction yielded 6% of TRS, exceptionally

202 low, signifying the catalyst for effective yield. Besides, hydrolysis without prior dissolution
203 resulted in 8% TRS yield. In this case, the low yield of TRS is due to solid-solid interactions of
204 cellulose substrate and H-ZSM-5. Prior dissolution of cellulose decreased the crystallinity and
205 degree of polymerization, which improved the H-ZSM-5 catalyst and the substrate's interaction.
206 In this condition, the dissolved MCC easily migrate to the catalyst's active surface to cause the
207 breakdown of the glycosidic bonds to release the sugar monomers. The higher conversion of
208 cellulose and maximum yield of TRS was obtained due to improved interaction of MCC substrate
209 with the catalyst.

210 Figure 3 shows, the hydrolysis of MCC and the effect of temperature on the yield of hydrolysis
211 products. The effectiveness of the hydrolysis of MCC in the catalytic effect of H-ZSM-5 in the
212 presence of [BMIM] Cl ionic liquid was studied based on TRS, glucose, fructose and 5-HMF yield.
213 The hydrolysis reaction results at the different temperatures indicated that the maximum yield of
214 TRS was obtained at 180 °C whereas for glucose the maximum yield was obtained at 190 °C. The
215 TRS yield showed an increase as temperature raised from 160 °C to 180 °C. However, the yield
216 showed a decreasing trend as temperature further increased due to the decomposition of TRS. As
217 seen in Figure 4, the hydrolysis of MCC is significantly affected by reaction temperature and time.
218 The results implied a maximum of 70% TRS comprising of 34% glucose, 8% fructose and 4.5%
219 5-HMF at a temperature of 180 °C and hydrolysis time of 180 min. Similarly, the effect of
220 hydrolysis time on the yield of TRS, glucose and fructose at different temperatures showed that
221 the product yield is significantly affected by reaction time. The yield of TRS increased with time
222 and reached a maximum of 180 min of hydrolysis time. Afterward, the TRS yield decreased due
223 to the decomposition of sugars because of extended reaction time. As can be observed from Figure
224 2, the depolymerization of cellulose using H-ZSM-5 catalyst in [BMIM] Cl ionic liquid results in

225 an increasing trend and decreases at extended time depolymerization. For cellulose hydrolysis
226 carried out for a run time of 180 min and at a catalyst to substrate ratio of 2:1 resulted in a sharp
227 increase in TRS yield as the temperature increased from 160 °C (44% yield of TRS) to 180 °C
228 (70% yield of TRS). However, further raising the temperature from 180 °C to 200 °C decreased the
229 yield to 60%. This is caused due to the decomposition of sugars such as glucose and fructose as
230 the temperature is increased above 180°C for 180 min of hydrolysis time.

231 For a comparative study, the experiments were carried out in a round bottom flask kept in an oil
232 bath. A typical experimental process is as follows: 0.1 g cellulose is dissolved in 2.0 g [BMIM] Cl
233 at predetermined dissolution temperature and time, and then a catalytic amount of H-ZSM-5
234 catalyst and 5ml of distilled water was added to the mixture. The Depolymerization of MCC was
235 carried out via two main steps; first through the prior dissolution of MCC in [BMIM] Cl ionic
236 liquid followed by hydrolysis by solid acid catalysts, H-ZSM-5 and Cr/H-ZSM-5. The purpose of
237 prior dissolution with [BMIM] Cl ionic liquid was to break the structural network of hydrogen
238 bonding in cellulose to achieve easier interaction between catalyst and substrate. Preliminary
239 experimental results were compared to the two catalysts for effective depolymerization of MCC
240 for further investigation. It was found that the H-ZSM-5 catalyst showed better catalytic activity
241 to depolymerize MCC a maximum yield of 70% total reducing sugar while the Cr/H-ZSM-5
242 catalyst yielded a maximum of 55%. However, Cr/H-ZSM-5 achieved a higher yield of 5-HMF
243 from fructose (53%) while H-ZSM-5 gives a maximum yield of 31% with identical reaction
244 condition. The weak catalytic activity Cr/H-ZSM-5 to depolymerize MCC to total reducing sugar
245 is due to a reduction in Bronsted acid sites due to chromium metal inclusion which generally
246 increases the Lewis acidity at the expense of Bronsted acid sites. For cellulose hydrolysis, higher

247 Bronsted acidity is required to cleave the glycosidic bond while for sugar dehydration, both
248 acidities' optimized acid sites play an essential role.

249 In transforming lignocellulosic biomass to value-added chemicals such as 5-HMF and LA, fructose
250 is considered the ideal substrate with more straightforward conversion and excellent yield of 5-
251 HMF using a wide range of homogeneous as well as heterogeneous catalysts. For instance,
252 chromium chloride (CrCl_2 , CrCl_3) and copper chloride catalysts in an ionic liquid have been
253 reported to be effective for dehydration of sugars to form 5-HMF with a maximum yield of 81%
254 from fructose and 70% using glucose [23][24]. However, the challenge in separation and the high
255 level of chromium toxicity hindered the practical production of 5-HMF. Heterogeneous acid
256 catalysts have easy recovery and production sustainability making them more promising for
257 practical applications in large-scale production than homogenous catalysts [25]. Therefore,
258 catalytic dehydration of fructose to 5-HMF using chromium metal impregnated on H-ZSM-5
259 support (5 % Cr/H-ZSM-5) was tested and the resulted in 87% conversion and 55% yield 5-HMF
260 in [BMIM] Cl-water reaction media. In this study with identical reaction condition, the yield of 5-
261 HMF using Cr/H-ZSM-5 catalyst was found to be effective compared with the yield obtained from
262 H-ZSM-5 catalyst (H-ZSM-5). Therefore, further investigation was carried out to study the effect
263 of temperature and dehydration time on 5-HMF yield.

264 The effect of temperature and reaction time on the dehydration of fructose catalyzed by Cr/H-
265 ZSM-5, using [BMIM] Cl-water as a solvent, has been studied. The yield of 5-HMF showed a
266 pattern of increasing and then decreasing with time at all temperatures studied. At 160 °C, the yield
267 of 5-HMF increased gradually to 34% up to 60 min, while at 180 °C it increased rapidly to 53%
268 after 30 min, showing that higher temperature increased the yield of 5-HMF and decreased the
269 dehydration time required. This was further confirmed at 200 °C with a of yield 47% 5-HMF at 15

270 min of dehydration time. The maximum yield was achieved at a temperature of 180 °C and 30 min
271 of reaction time. When the dehydration reaction time was extended over 30 min, the yield of 5-
272 HMF decreased significantly due to decomposition of 5-HMF. The degradation products contain
273 levulinic acid, formic acid and soluble polymers as observed from HPLC analysis. However, the
274 separated products were exceedingly small to be quantified. In the case of soluble polymers, a
275 wide range of products are possibly available, which is very difficult to obtain the accurate
276 molecular structure and determine the exact product type [25].

277 The reaction temperature and time have a significant influence on the conversion of glucose to 5-
278 HMF. The conversion of glucose to 5-HMF at a temperature of 200 °C and 60 min of reaction
279 time yielding a maximum yield of 24% 5-HMF was achieved. The results suggested that as
280 temperature increased, the yield of 5-HMF also increased initially and then followed a decreasing
281 pattern at extended reaction time due to the formation of undesired products such as insoluble
282 humin and soluble polymers [26]. Moreover, the formation of 5-HMF from glucose at 160°C and
283 180°C at 120 min of reaction time resulted in maximum yield of 17 and 19.5% HMF, respectively.
284 The dehydration of glucose is relatively complex compared with fructose due to the six-membered
285 pyranoside structure. For this reason, the dehydration of glucose to 5-HMF undergoes an additional
286 step of isomerization of glucose to fructose before the dehydration reaction to form 5-HMF using
287 Cr/H-ZSM-5 catalyst.

288 **3.2.3 Mechanism of MCC Hydrolysis**

289 During the hydrolysis of MCC, two steps are essential: the dissolution of MCC in [BMIM] Cl
290 ionic liquid and subsequent hydrolysis in the presence of water as a co-solvent using catalytic
291 amount of H-ZSM-5 catalyst. The purpose of dissolution of MCC alone in the ionic liquid is

292 primarily to overcome cellulose's recalcitrant behavior and break the hydrogen bonding
293 networking in the cellulose strand. This step is essential to improve the accessibility of β -1, 4-
294 glycosidic linkages between the glucose and create contact between the substrate and catalyst
295 within the reaction media. Besides, prior dissolution helps simplify the structural complexity of
296 cellulose resulting from higher crystallinity and a more significant degree of cellulose
297 polymerization to ease hydrolysis. Mechanistically, the chlorine ions of the ionic liquid are
298 efficient in forming a new hydrogen bonding with the hydroxyl groups of cellulose while the
299 cations prevent the crosslinking of cellulose in the dissolution process. The cations form a linkage
300 with the oxygen of the broken hydroxyl groups of the cellulose and serve as electron acceptors
301 (Figure 6).

302 The hydrolysis of MCC is described by the Saeman model [27] that the reaction kinetics follows
303 two pseudo-homogeneous consecutive first-order reaction. The degradation products are mainly
304 5-HMF and humins. The Mechanism of MCC hydrolysis over H-ZSM-5 catalyst is like the
305 hydrolysis of cellulose in the presence of homogeneous acidic catalysts such as sulphuric acids.
306 The glycosidic bonds in cellulose polymer are broken by Bronsted acid sites similar to H^+ ions of
307 acidic solution breaks the bond to release the glucose monomers through binding with the
308 glycosidic oxygen atom leading to hydrolysis of MCC to simple sugars. H^+ cations generated in-
309 situ from the Bronsted acid sites of zeolite were the key active species for the effective hydrolysis
310 of cellulose over H-ZSM-5 and the Lewis acid sites do not exhibit high activity as reported from
311 FT-IR through pyridine adsorption [19]. In addition to the catalyst, the H^+ molecules produced
312 from the dissociation of water (co-solvent) participate in the hydrolysis reaction, facilitating the
313 glycosidic bond's cleavage.

314 **3.2.3 Kinetic modeling of MCC depolymerization**

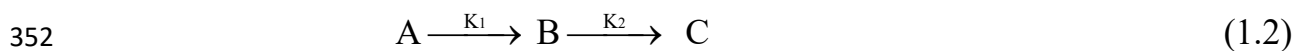
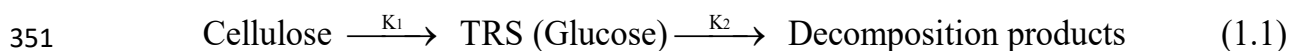
315 Valorization of lignocellulosic biomass requires understanding the mechanism and kinetics of the
316 complex cellulose hydrolysis reaction [28]. The complexity of cellulose hydrolysis emerged from
317 the recalcitrant behavior of cellulose which requires harsh reaction conditions. The hydrolysis
318 products (sugars) have high reactivity that suffers from further decomposition at severe reaction
319 conditions. The incompatibility between the cellulose stability and highly reactive hydrolysis
320 products complicates understanding the reaction mechanism and kinetics of cellulose hydrolysis.
321 However, understanding the mechanism and kinetics of hydrolysis reaction is especially important
322 for process design and optimization. The kinetic modeling for cellulose hydrolysis in the
323 synergetic effect of H-ZSM-5 catalyst and [BMIM] Cl ionic liquid has been studied to investigate
324 the ionic liquid's effect on the rate of reaction, activation energy and mechanism of hydrolysis.

325 The yield data of TRS were obtained experimentally and data generated from the mathematical
326 model (Eqn 1.4), the activation energy and reaction rate constants (k_1 and k_2) were calculated and
327 compared, and the results are presented in Figure 3. The experiments were performed over a wide
328 temperature range (140 to 200 °C) and hydrolysis run time (0 to 180 min). The kinetic model used
329 is a model developed by Saeman for cellulose hydrolysis, and the present study assumes
330 irreversible pseudo-homogeneous first-order reactions [27]. The estimate of the kinetic parameters
331 is performed using Polymath 6.0 software. The following assumptions were taken into
332 consideration for model development:

- 333 1. The first step in depolymerization of microcrystalline cellulose is the cleavage of β -(1, 4)
334 glycosidic bonds followed by decomposition of TRS to other products 5-HMF and humin.
- 335 2. The reaction rate equations were developed based on the Saeman model considering all the
336 model's assumptions [27].

- 337 3. The TRS concentration was based on MCC's hydrolysis reaction that includes the major
 338 depolymerization products intermediate sugars and oligomers.
- 339 4. Mass transfer on the reaction kinetics was insignificant due to the complete dissolution of
 340 cellulose in [BMIM] Cl ionic liquid media before depolymerization reaction.
- 341 5. It is assumed that dissolved cellulose diffuses into the internal pores of zeolite and the
 342 glycosidic bonds of cellulose then extend into the vicinity of Bronsted acid sites where catalytic
 343 depolymerization takes place [29].

344 Hydrolysis of lignocellulosic biomass is an overly complex reaction comprising of formation and
 345 decomposition of sugars. Therefore, a simplified kinetic model is used to describe the formation
 346 and decomposition of sugar products from cellulose's hydrolysis. The model proposes that
 347 cellulose depolymerization involves the hydrolysis of cellulose to reducing sugar and subsequent
 348 degradation of sugar to furan chemicals and humin. The reaction scheme for depolymerization of
 349 cellulose is shown in Equation 1.1 while the reaction rate constant for thesecond series reaction
 350 i.e., TRS decomposition is given in Equation 1.2.



353 The formation rate of reducing sugars (B) with respect to depolymerization time is represented by
 354 Equation 1.4. The integration of Equation 1.4 (considering the following boundary conditions at t
 355 =0, C_{B,0} = 0) with respect to time gives Equation 1.6 which was used to represent the concentration
 356 of total reducing sugar production as a function of time and used to calculate the reaction constants
 357 (k₁ (min⁻¹) and k₂ (min⁻¹)). The Arrhenius equation describes the correlation of reaction rate
 358 constants with the temperature. The activation energies were calculated from the Arrhenius

359 equations with a reference temperature. For a batch reaction rate of formation of the reactions is
360 given as follow:

$$361 \quad -r_A = k_1 C_A \quad (1.3)$$

$$362 \quad r_B = k_1 C_A - k_2 C_B \quad (1.4)$$

$$363 \quad r_C = k_1 C_A \quad (1.5)$$

364 The concentration of TRS with time can be calculated as shown in Eqn 1.6 below:

$$365 \quad C_B = k_1 C_{A0} \left(\frac{e^{-k_1 t} - e^{-k_2 t}}{k_2 - k_1} \right) \quad (1.6)$$

366 Where C_A is the cellulose concentration (mg ml^{-1}), C_{A0} is the initial concentration of cellulose (mg
367 ml^{-1}), C_B is the total reducing sugars concentration (mg ml^{-1}), C_C is decomposition product
368 concentration and 't' is the depolymerization reaction time (min).

369 **3.2.3 Formation and Degradation of TRS**

370 The application of ionic liquid for catalytic hydrolysis of cellulose to value-added chemicals is a
371 promising approach to overcome the recalcitrant nature of cellulose for a potential scale-up to the
372 bio-refinery scheme. The presence of [BMIM] Cl ionic liquid improved the yield of interest
373 products from microcrystalline cellulose's depolymerization. The role [BMIM] Cl was significant
374 mainly for three reasons: (1) [BMIM] Cl dissolved cellulose entirely within the given substrate
375 loading, (2) the chloride ions in the ionic liquid played the role of base and nucleophile that
376 promoted the isomerization of glucose to fructose and (3) [BMIM]⁺ of the ionic liquid stabilize
377 dehydration products from further decomposition [30]. Dissolution temperature and time showed

378 a profound effect on reducing the crystallinity index and degree of cellulose polymerization.
379 Higher the crystallinity and degree of polymerization of cellulose, the less the reactivity to
380 depolymerize to sugar monomers. Therefore, it is imperative to dissolve cellulose and reduce its
381 crystallinity to hydrolyze the substrate effectively. The reduction in crystallinity was achieved
382 through the prior dissolution of cellulose in an ionic liquid followed by the hydrolysis reaction
383 using the catalytic effect of the H-ZSM-5 catalyst.

384 A kinetic model was constructed based on calculating the best-fit reaction coefficients for k_1 and
385 k_2 , as presented in Table 2. The model fitted well with the experimental data for all four temperature
386 sets with an R^2 value greater than 0.96 showing reasonable agreement between the experimental
387 and calculated data. Figure 7 shows the kinetic data and compared with the experimental result. It
388 is observed that the activation energies of formation and decomposition of sugars decreased
389 significantly for [BMIM] Cl ionic liquid media compared with the hydrolysis that takes place in
390 aqueous media [31]. The activation energy of cellulose depolymerization to reducing sugars
391 calculated ($E_{a1} = 85.8 \text{ kJ mol}^{-1}$), is less than the calculated activation energy for acid hydrolysis of
392 cellulose in water ($E_{a1} = 105 - 188 \text{ kJ mol}^{-1}$) [9]. The activation energy values reported in cellulose
393 hydrolysis using ionic liquid solvent falls in the range of 55 to 89 kJ mol^{-1} which depends on the
394 nature of the ionic liquid and the co-solvent effect [10].

395 Similarly, the activation energy for decomposition of reducing sugars in ionic liquid was lower
396 ($E_{a2} = 42.5 \text{ kJ mol}^{-1}$) than aqueous media ($E_{a2} = 120 \text{ kJ mol}^{-1}$). The decrease in activation
397 energies for the consecutive reactions can be attributed to the ionic liquid's ionic nature, enhancing
398 the susceptibility of glycosidic bond cleavage to release the sugar monomers. The plot of $\ln(k)$ vs.
399 $1/T$ leads to a straight line with a slope of the fitting line indicating the activation energy and pre-
400 exponential factor is determined by the intercept of the fitting curve as shown in Figure 8 and

401 reported in the literature [32] for both formation and decomposition of reducing sugar from the
402 depolymerization of cellulose.

403 **4. Conclusion** The inert nature of cellulose and insufficient knowledge in solid-solid reaction
404 systems make the heterogeneous catalytic conversion of cellulose ambitious. In our research,
405 porous zeolite materials (H-ZSM-5) and ionic liquid have shown extraordinary ability to perform
406 as catalyst and catalyst support for cellulose conversion. It appears that the mechanism of action
407 of the zeolite catalyst is via the breaking of the glycosidic bonds in cellulose to release the glucose
408 monomers. The closeness of the acidic sites may be essential for cellulose hydrolysis than acidic
409 strength alone.

410 A kinetic study for MCC hydrolysis using the synergistic effect of [BMIM] Cl ionic liquid was
411 performed over H-ZSM-5. The catalyst was adequate for the MCC's depolymerization up to a yield
412 value of 70% TRS. [BMIM] Cl ionic liquid was highly influential in overcoming cellulosic
413 biomass's recalcitrance by breaking the extensive network of intra and inter-hydrogen bonding and
414 the strong acidity of H-ZSM-5 was able to break the beta-1, 4-glycosidic bond to release sugar
415 molecules. During depolymerization reaction, ionic liquid's presence significantly reduced the
416 activation energy of both the formation and decomposition of sugar obtained from the reaction.
417 The activation energy calculated in cellulose hydrolysis using H-ZSM-5 for a depolymerization
418 time of 180 min was found to be 85.8 kJ mol⁻¹ while the decomposition of reducing sugars in
419 ionic liquid was found to be 42.5 kJ mol⁻¹. **Reference**

420 [1] R. J. Chimentão, E. Lorente, F. Gispert-Guirado, F. Medina, and F. López, “Hydrolysis of
421 dilute acid-pretreated cellulose under mild hydrothermal conditions,” *Carbohydr. Polym.*,
422 vol. 111, pp. 116–124, 2014, doi: 10.1016/j.carbpol.2014.04.001.

- 423 [2] W. Ji, Z. Shen, and Y. Wen, “Hydrolysis of wheat straw by dilute sulfuric acid in a
424 continuous mode,” *Chem. Eng. J.*, vol. 260, pp. 20–27, 2015, doi:
425 10.1016/j.cej.2014.08.089.
- 426 [3] T. Auxenfans, S. Buchoux, K. Djellab, C. Avondo, E. Husson, and C. Sarazin, “Mild
427 pretreatment and enzymatic saccharification of cellulose with recycled ionic liquids towards
428 one-batch process,” *Carbohydr. Polym.*, vol. 90, no. 2, pp. 805–813, 2012, doi:
429 10.1016/j.carbpol.2012.05.101.
- 430 [4] Y. Chen, G. Li, F. Yang, and S. Zhang, “Mn / ZSM-5 participation in the degradation of
431 cellulose under phosphoric acid media,” *Polym. Degrad. Stab.*, vol. 96, no. 5, pp. 863–869,
432 2011, doi: 10.1016/j.polymdegradstab.2011.02.007.
- 433 [5] C. Abels, K. Thimm, H. Wulforth, A. Christine, and M. Wessling, “Bioresource
434 Technology Membrane-based recovery of glucose from enzymatic hydrolysis of ionic
435 liquid pretreated cellulose,” *Bioresour. Technol.*, vol. 149, pp. 58–64, 2013, doi:
436 10.1016/j.biortech.2013.09.012.
- 437 [6] J. Wang, J. Xi, and Y. Wang, “Recent advances in the catalytic production of glucose from
438 lignocellulosic biomass,” *Green Chem.*, vol. 17, no. 2, pp. 737–751, 2015, doi:
439 10.1039/C4GC02034K.
- 440 [7] J. Verendel, T. Church, and P. Andersson, “Catalytic One-Pot Production of Small Organics
441 from Polysaccharides,” *Synthesis (Stuttg.)*, vol. 2011, no. 11, pp. 1649–1677, Apr. 2011,
442 doi: 10.1055/s-0030-1260008.
- 443 [8] H. T. Vo, V. T. Widyaya, J. Jae, H. S. Kim, and H. Lee, “Hydrolysis of ionic cellulose to
444 glucose,” *Bioresour. Technol.*, vol. 167, pp. 484–489, 2014, doi:

- 445 10.1016/j.biortech.2014.06.025.
- 446 [9] Y.-B. Huang and Y. Fu, “Hydrolysis of cellulose to glucose by solid acid catalysts,” *Green*
447 *Chem.*, vol. 15, no. 5, p. 1095, 2013, doi: 10.1039/c3gc40136g.
- 448 [10] A. Brandt, J. Gräsvik, J. P. Hallett, and T. Welton, “Deconstruction of lignocellulosic
449 biomass with ionic liquids,” *Green Chem.*, vol. 15, no. 3, pp. 550–583, 2013, doi:
450 10.1039/c2gc36364j.
- 451 [11] Y. Fukaya, K. Hayashi, and H. Ohno, “Cellulose dissolution with polar ionic liquids under
452 mild conditions: required factors for anions {,” no. Chart 1, pp. 44–46, 2008, doi:
453 10.1039/b713289a.
- 454 [12] X. Tong, Y. Ma, and Y. Li, “Applied Catalysis A: General Biomass into chemicals: :
455 Conversion of sugars to furan derivatives by catalytic processes,” *Applied Catal. A, Gen.*,
456 vol. 385, no. 1–2, pp. 1–13, 2010, doi: 10.1016/j.apcata.2010.06.049.
- 457 [13] S. Kassaye, C. Pagar, K. K. Pant, S. Jain, and R. Gupta, “Bioresource Technology
458 Depolymerization of microcrystalline cellulose to value added chemicals using sulfate ion
459 promoted zirconia catalyst,” *Bioresour. Technol.*, vol. 220, pp. 394–400, 2016, doi:
460 10.1016/j.biortech.2016.08.109.
- 461 [14] X. Cao *et al.*, “Impact of regeneration process on the crystalline structure and enzymatic
462 hydrolysis of cellulose obtained from ionic liquid.,” *Carbohydr. Polym.*, vol. 111, pp. 400–
463 3, Oct. 2014, doi: 10.1016/j.carbpol.2014.05.004.
- 464 [15] P. K. Rout, A. D. Nannaware, O. Prakash, A. Kalra, and R. Rajasekharan, “Synthesis of
465 hydroxymethylfurfural from cellulose using green processes: A promising biochemical and

- 466 biofuel feedstock,” *Chem. Eng. Sci.*, vol. 142, pp. 318–346, 2016, doi:
467 10.1016/j.ces.2015.12.002.
- 468 [16] S. Kassaye, K. K. Pant, and S. Jain, “Synergistic effect of ionic liquid and dilute sulphuric
469 acid in the hydrolysis of microcrystalline cellulose,” *Fuel Process. Technol.*, vol. 148, pp.
470 289–294, 2016, doi: 10.1016/j.fuproc.2015.12.032.
- 471 [17] H. E. van der Bij and B. M. Weckhuysen, “Local silico-aluminophosphate interfaces within
472 phosphated H-ZSM-5 zeolites.,” *Phys. Chem. Chem. Phys.*, vol. 16, no. 21, pp. 29–32, 2014,
473 doi: 10.1039/c3cp54791d.
- 474 [18] N. Mimura, M. Okamoto, H. Yamashita, S. T. Oyama, and K. Murata, “Oxidative
475 dehydrogenation of ethane over Cr/ZSM-5 catalysts using CO₂ as an oxidant.,” *J. Phys.
476 Chem. B*, vol. 110, no. 43, pp. 21764–70, 2006, doi: 10.1021/jp061966l.
- 477 [19] H. Cai, C. Li, A. Wang, G. Xu, and T. Zhang, “Applied Catalysis B : Environmental Zeolite-
478 promoted hydrolysis of cellulose in ionic liquid , insight into the mutual behavior of zeolite
479 , cellulose and ionic liquid,” *Applied Catal. B, Environ.*, vol. 123–124, pp. 333–338, 2012,
480 doi: 10.1016/j.apcatb.2012.04.041.
- 481 [20] H. Liu, H. Wei, W. Xin, and C. Song, “Differences between Zn / HZSM-5 and Zn / HZSM-
482 11 zeolite catalysts in alkylation of benzene with dimethyl ether,” *J. Energy Chem.*, vol. 23,
483 no. 5, pp. 617–624, 2014, doi: 10.1016/S2095-4956(14)60192-3.
- 484 [21] A. M. Santa Arango, C. M. Escobar Garcés, J. L. Agudelo Valderrama, A. Guzmán
485 Monsalve, L. A. Palacio Santos, and A. Echavarría Isaza, “Oligomerization of propene over
486 ZSM-5 modified with Cr and W,” *Rev. Fac. Ing.*, no. 57, pp. 57–65, 2011.

- 487 [22] I. G. Baek, S. J. You, and E. D. Park, "Bioresource Technology Direct conversion of
488 cellulose into polyols over Ni / W / SiO₂ -Al₂O₃," *Bioresour. Technol.*, vol. 114, pp.
489 684–690, 2012, doi: 10.1016/j.biortech.2012.03.059.
- 490 [23] S. Bali, M. A. Tofanelli, R. D. Ernst, and E. M. Eyring, "Chromium (III) catalysts in ionic
491 liquids for the conversion of glucose to 5- (hydroxymethyl) furfural (HMF): Insight into
492 metal catalyst : ionic liquid mediated conversion of cellulosic biomass to biofuels and
493 chemicals," *Biomass and Bioenergy*, vol. 42, no. Iii, pp. 224–227, 2012, doi:
494 10.1016/j.biombioe.2012.03.016.
- 495 [24] H. Zhao, J. E. Holladay, H. Brown, and Z. C. Zhang, "Reports 8.," vol. 113409, no. 2005,
496 2006.
- 497 [25] H. Xu *et al.*, "Dehydration of fructose into 5-hydroxymethylfurfural by high stable ordered
498 mesoporous zirconium phosphate," *Fuel*, vol. 145, pp. 234–240, 2015, doi:
499 10.1016/j.fuel.2014.12.072.
- 500 [26] L. Hu, Z. Wu, J. Xu, Y. Sun, L. Lin, and S. Liu, "Zeolite-promoted transformation of
501 glucose into 5-hydroxymethylfurfural in ionic liquid," *Chem. Eng. J.*, vol. 244, pp. 137–
502 144, 2014, doi: 10.1016/j.cej.2014.01.057.
- 503 [27] J. F. Saeman, "Hydrolysis of Cellulose and Decomposition of Sugars in Dilute Acid at High
504 Temperature," *Ind. Eng. Chem.*, vol. 37, no. 9, pp. 43–52, 1945, doi: Doi
505 10.1021/Ie50421a009.
- 506 [28] L. Negahdar, I. Delidovich, and R. Palkovits, "Aqueous-phase hydrolysis of cellulose and
507 hemicelluloses over molecular acidic catalysts: Insights into the kinetics and reaction
508 mechanism," *Appl. Catal. B Environ.*, vol. 184, pp. 285–298, 2016, doi:

509 10.1016/j.apcatb.2015.11.039.

510 [29] F. Guo, Z. Fang, C. C. Xu, and R. L. Smith, “Solid acid mediated hydrolysis of biomass for
511 producing biofuels,” *Prog. Energy Combust. Sci.*, vol. 38, no. 5, pp. 672–690, 2012, doi:
512 10.1016/j.peccs.2012.04.001.

513 [30] L. Hu *et al.*, “Catalytic conversion of carbohydrates into 5-hydroxymethylfurfural over
514 cellulose-derived carbonaceous catalyst in ionic liquid,” *Bioresour. Technol.*, vol. 148, pp.
515 501–7, Nov. 2013, doi: 10.1016/j.biortech.2013.09.016.

516 [31] A. J. Kunov-Kruse, A. Riisager, S. Saravanamurugan, R. W. Berg, S. B. Kristensen, and R.
517 Fehrmann, “Revisiting the Bronsted acid catalysed hydrolysis kinetics of polymeric
518 carbohydrates in ionic liquids by in situ ATR-FTIR spectroscopy,” *Green Chem.*, vol. 15,
519 no. 10, pp. 2843–2848, 2013, doi: 10.1039/c3gc41174e.

520 [32] M. Mohan, T. Banerjee, and V. V Goud, “Hydrolysis of bamboo biomass by subcritical
521 water treatment,” *Bioresour. Technol.*, vol. 191, pp. 244–252, 2015, doi:
522 10.1016/j.biortech.2015.05.010.

523

Table 1. BET surface area analysis of H-ZSM-5 and Cr/H-ZSM-5 catalysts

Catalyst Type	BET surface area (m²/g)
H-ZSM-5	270.0
Cr/H-ZSM-5	248.2

Table 2. Kinetic rate constants at different temperatures

Temperature (°C)	k ₁ (min ⁻¹)	k ₂ (min ⁻¹)
140	0.0010	0.0006
160	0.0042	0.0019
180	0.0094	0.0020
200	0.0244	0.0035

Figures

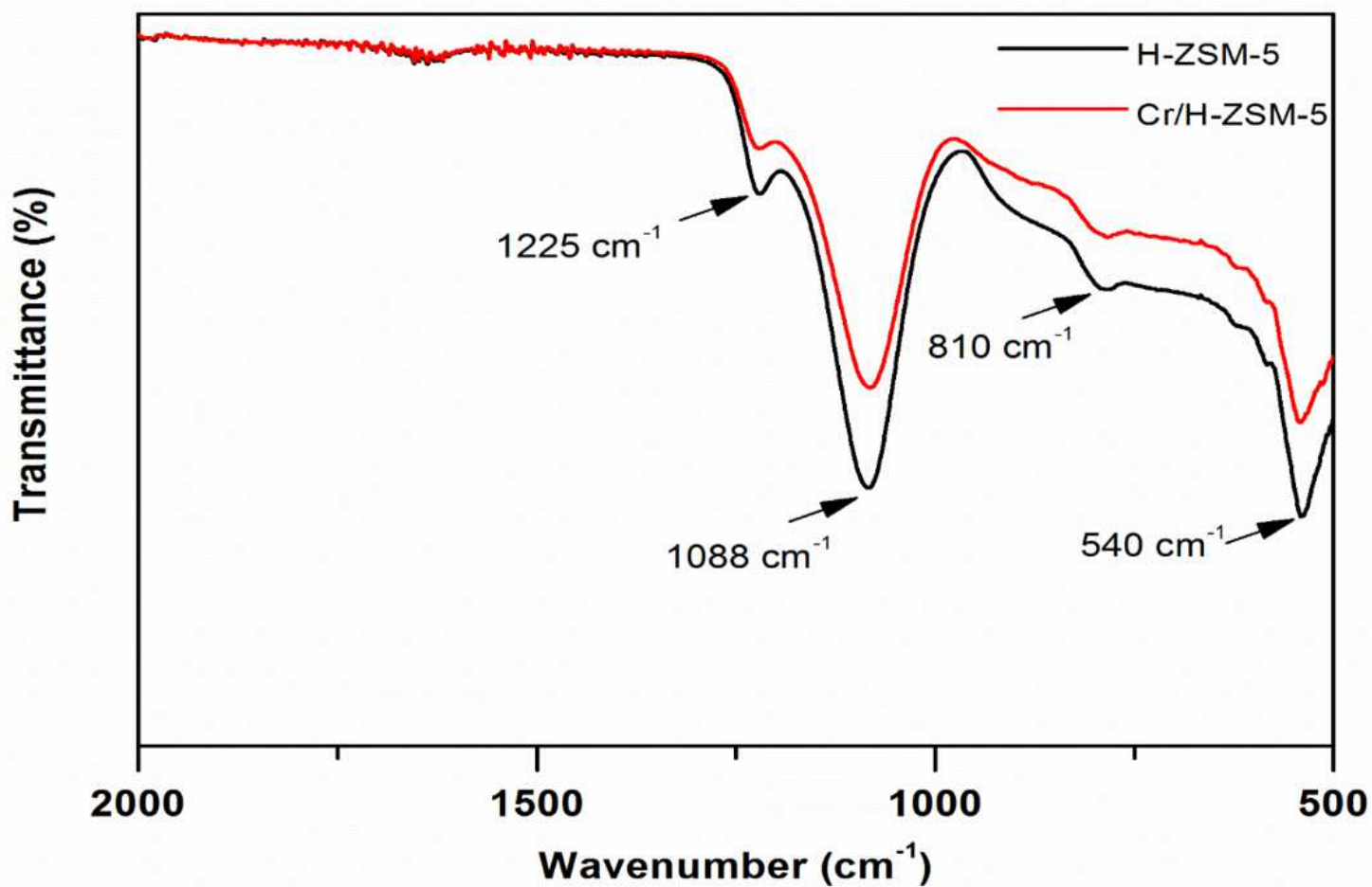


Figure 1

FTIR analysis of H-ZSM-5 and Cr/H-ZSM-5 catalysts

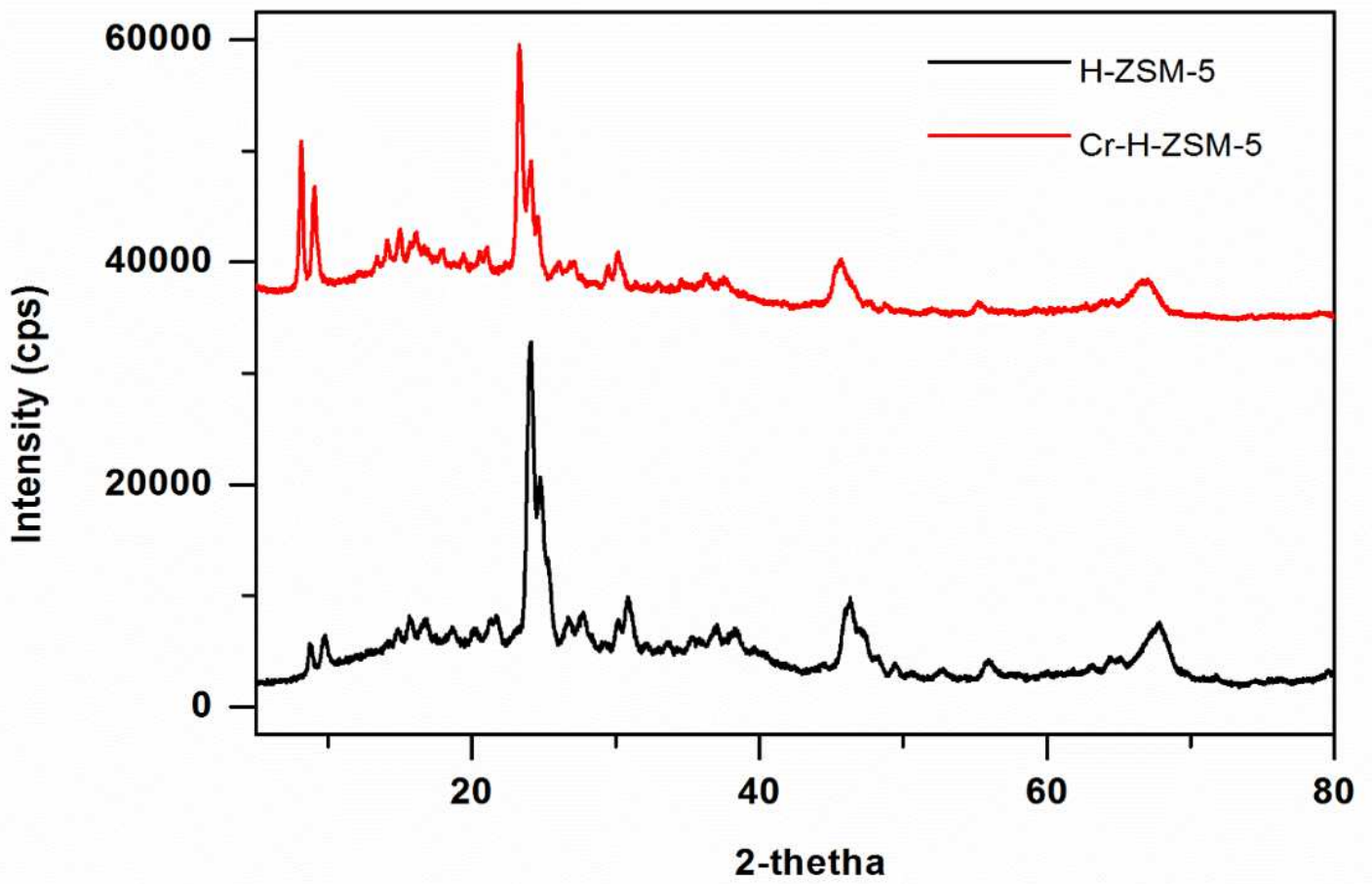


Figure 2

XRD pattern of H-ZSM-5 and Cr/H-ZSM-5 catalysts

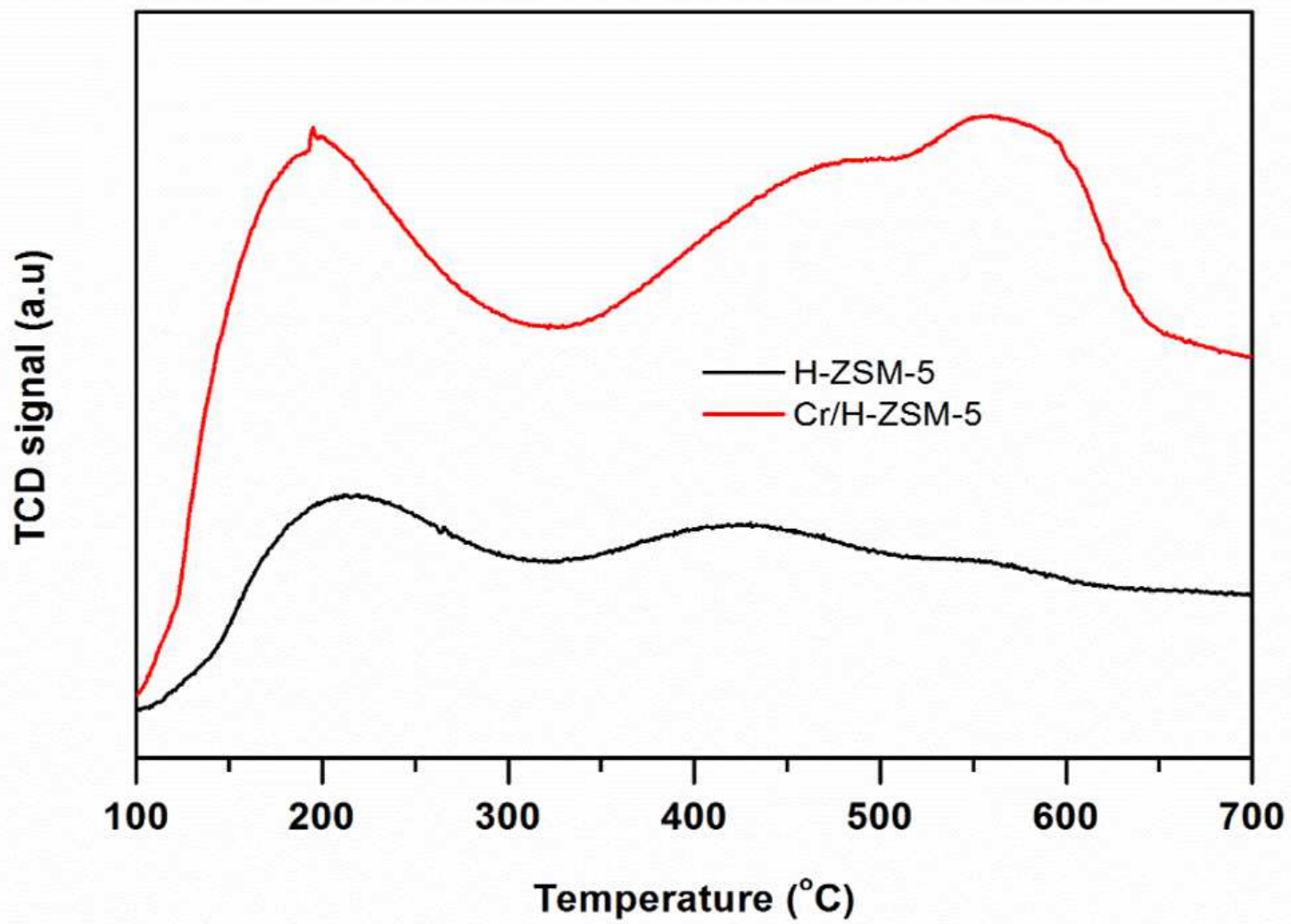


Figure 3

Ammonia-TPD analysis of H-ZSM-5 and Cr/H-ZSM-5 catalysts

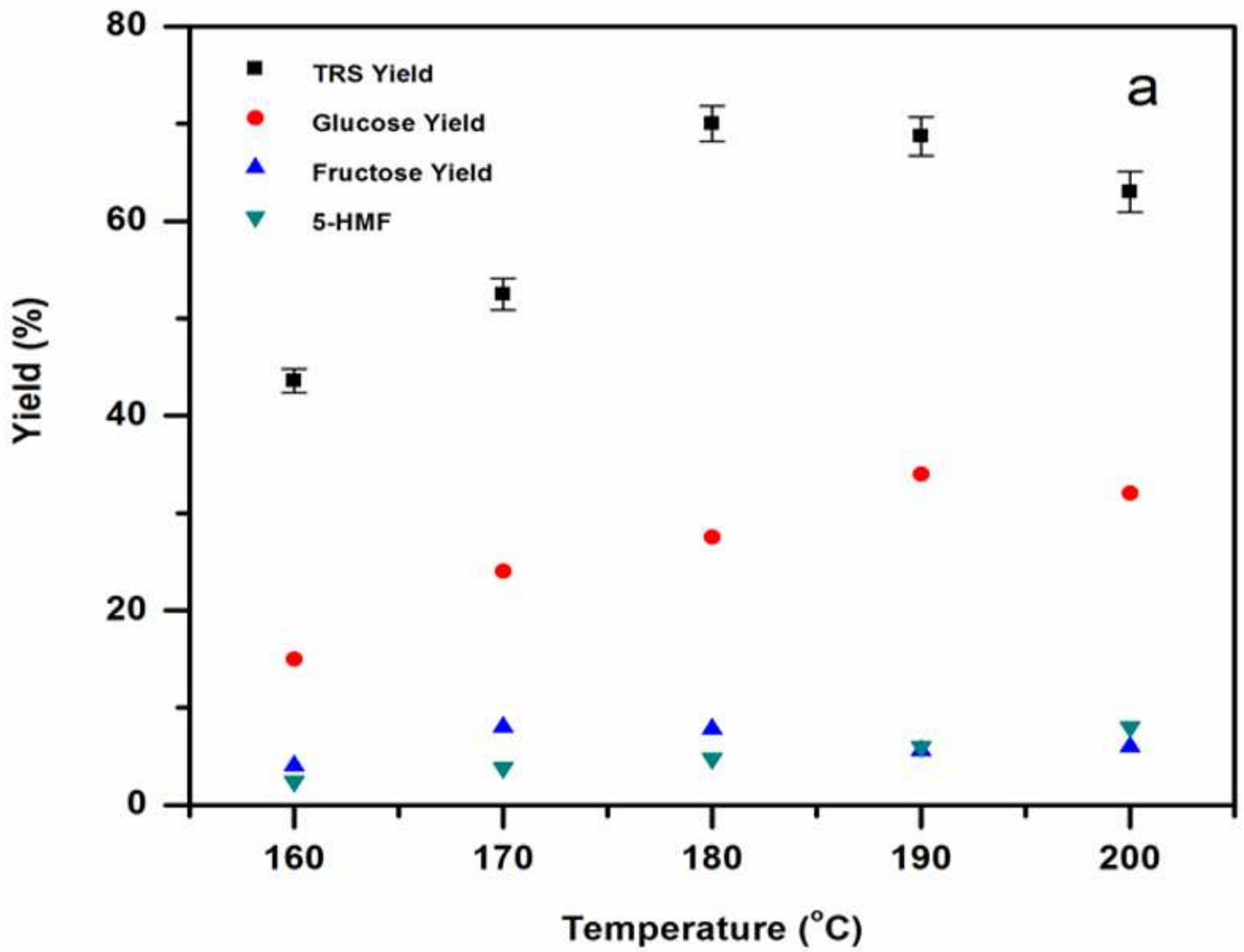


Figure 4

Effect of hydrolysis temperature on TRS yield (catalyst to substrate ratio of 2:1 (w/w) and 180 min of reaction time)

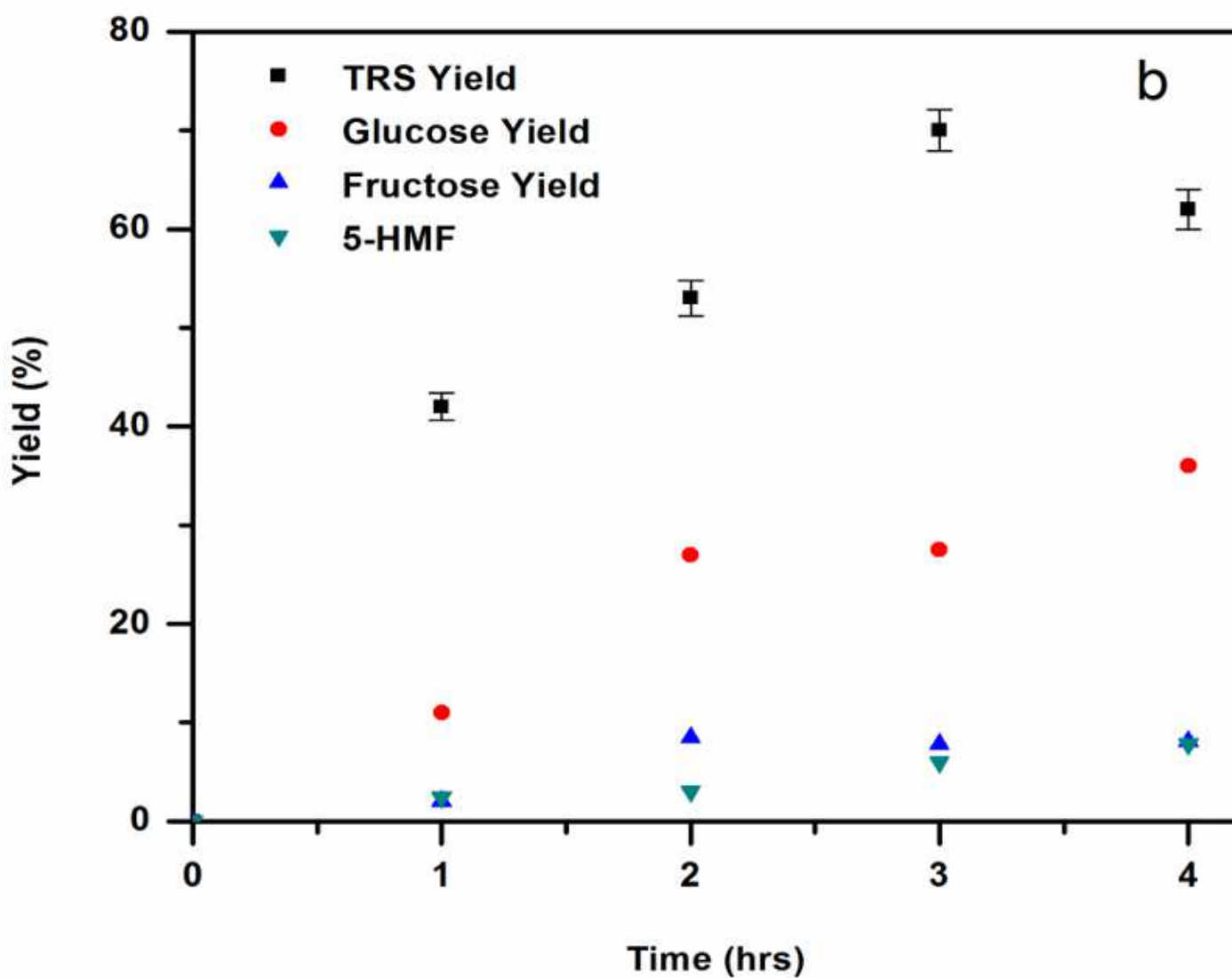


Figure 5

Effect of hydrolysis time on yield of TRS (temperature 180 oC, catalyst to substrate ratio of 2:1 (w/w))

1-Butyl-3-methylimidazolium chloride

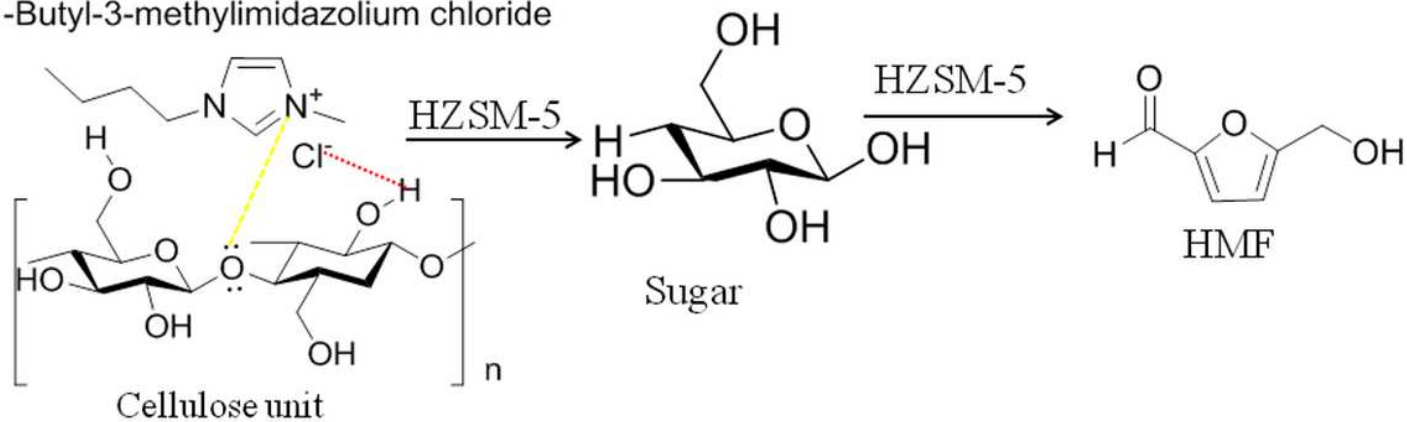


Figure 6

Mechanism of Cellulose Hydrolysis over H-ZSM-5 catalyst in the presence of [BMIM] Cl ionic liquid

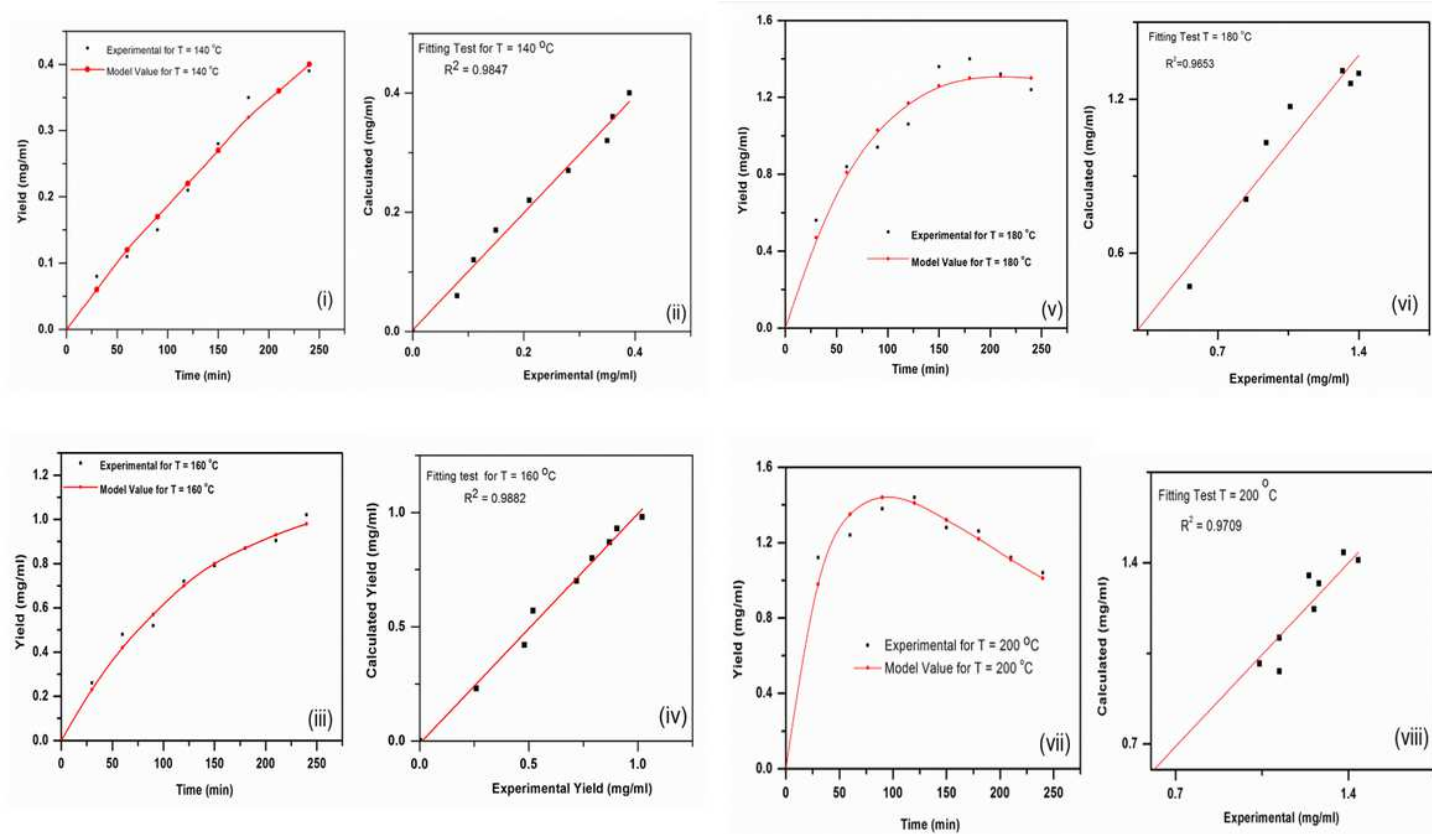


Figure 7

Kinetic modelling of cellulose hydrolysis using H-ZSM-5 catalyst in [BMIM] Cl-water media

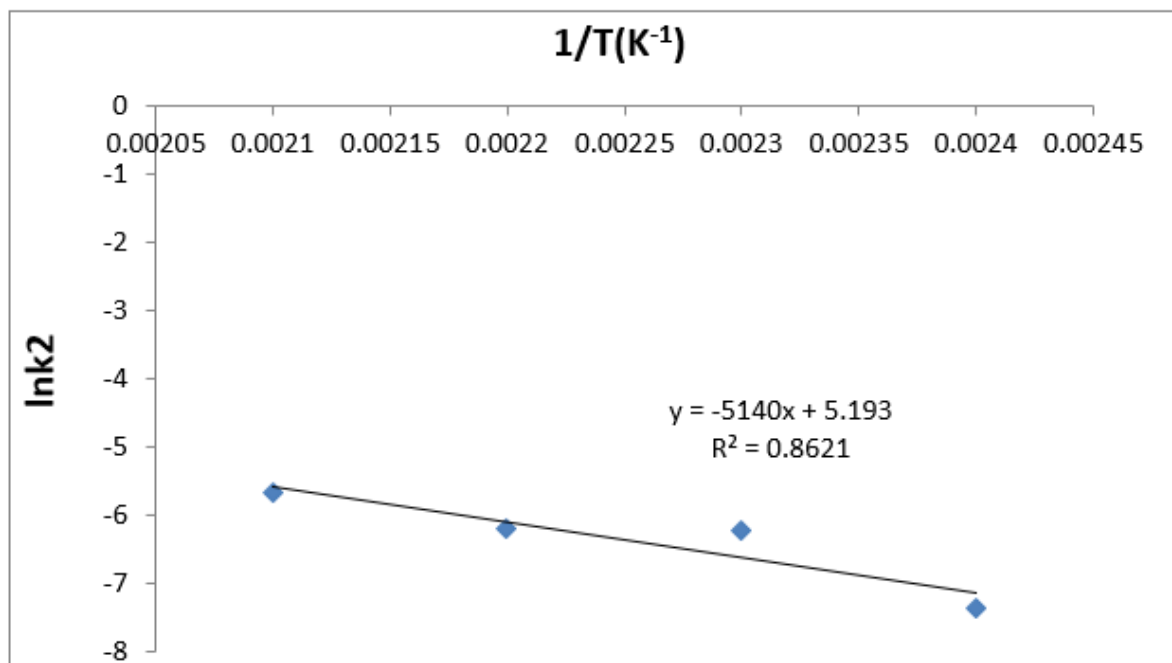
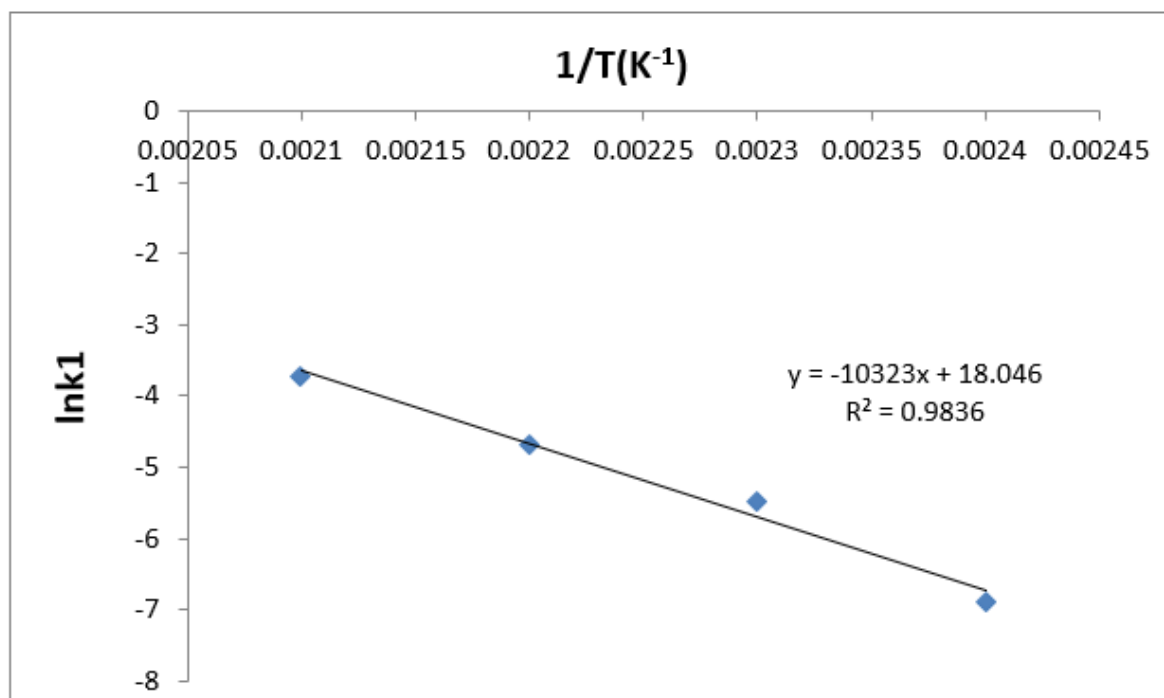


Figure 8

Determination of rate constants for cellulose hydrolysis using H-ZSM-5 catalyst in [BMIM] Cl